Hindawi
Journal of Analytical Methods in Chemistry
Volume 2018, Article ID 1651989, 5 pages
https://doi.org/10.1155/2018/1651989

Research Article

A Pyridazine-Based Fluorescent Probe Targeting Aβ Plaques in Alzheimer's Disease

Yong Dae Park,[1] **Jeum-Jong Kim**,[2] **Sungbeom Lee**,[1] **Chul-Hong Park**,[1] **Hyoung-Woo Bai**,[1] **and Seung Sik Lee**[1]

[1]*Research Division for Biotechnology, Advanced Radiation Technology Institute, Korea Atomic Energy Research Institute, Jeongeup 580-185, Republic of Korea*
[2]*Technology Innovation Support Team, Korea Research Institute of Chemical Technology (KRICT), Deajeon 305-600, Republic of Korea*

Correspondence should be addressed to Yong Dae Park; ydpark@kaeri.re.kr

Received 10 October 2017; Accepted 14 December 2017; Published 27 February 2018

Academic Editor: Subhankar Singha

Accumulation of β-amyloid (Aβ) plaques comprising Aβ40 and Aβ42 in the brain is the most significant factor in the pathogenesis of Alzheimer's disease (AD). Thus, the detection of Aβ plaques has increasingly attracted interest in the context of AD diagnosis. In the present study, a fluorescent pyridazine-based dye that can detect and image Aβ plaques was designed and synthesized, and its optical properties in the presence of Aβ aggregates were evaluated. An approximately 34-fold increase in emission intensity was exhibited by the fluorescent probe after binding with Aβ aggregates, for which it showed high affinity ($K_D = 0.35\ \mu M$). Moreover, the reasonable hydrophobic properties of the probe ($\log P = 2.94$) allow it to penetrate the blood brain barrier (BBB). In addition, the pyridazine-based probe was used in the histological costaining of transgenic mouse (APP/PS1) brain sections to validate the selective binding of the probe to Aβ plaques. The results suggest that the pyridazine-based compound has the potential to serve as a fluorescent probe for the diagnosis of AD.

1. Introduction

The misfolding and aggregation of proteins cause numerous neurodegenerative diseases, such as Alzheimer's disease (AD), prion disease (PrD), and Parkinson's disease (PD) [1]. AD, one of the most common protein misfolding diseases (PMDs), is characterized by the accumulation of misfolded β-amyloid (Aβ) peptides and neurofibrillary tangles (NFTs) containing tau protein in the brain. A recent report revealed that the buildup of Aβ plaques in the brain plays a significant role in the pathogenesis of AD [2, 3]. Therefore, approaches to visualize Aβ deposition might prove useful for diagnosing AD and evaluating the efficacy of AD therapeutics [4–6].

Several groups have reported novel positron emission tomography (PET) imaging agents targeting Aβ plaques to diagnose AD, including BAY94-9172, FDDNP, PIB, SB-13, AV-45, and IMPY [7–13]. However, these agents are hindered by factors such as long data acquisition processes, costly equipment, exposure to radioactivity, need for proficient personnel, and comparatively poor spatial resolution [14]. Interest in monitoring the progression of AD by imaging Aβ plaques using fluorescence spectroscopy has also increased [15, 16]. Compared to nuclear imaging methods, fluorescence imaging has many advantages, including providing real-time, nonradioactive, inexpensive, and high-resolution imaging, both in vivo and ex vivo. Consequently, various fluorescent probes for imaging Aβ plaques have been developed [17–22]. An excellent fluorescent probe for Aβ plaques must meet the following requirements [18, 21, 23]: (1) selective targeting of Aβ plaques, (2) acceptable lipophilicity ($\log P$ value between 1 and 3), (3) high-affinity binding, (4) straightforward synthesis, and (5) a significant change in fluorescent properties upon binding to Aβ deposits.

Based on these requirements, we developed and reported fluorescent pyridazine probes targeting Aβ plaques [24].

These pyridazine probes can be used for imaging through selective binding but lack the required binding affinity for Aβ plaques. Here, we describe the optimization of pyridazine derivatives based on the conjugation of an electron acceptor with an electron donor.

To optimize these fluorescent probes, the electron-donating *p*-dimethylamino group and electron-accepting cyano group were introduced to construct a compound with a donor-π-acceptor structure (Figure 1). In this paper, we describe the synthesis and optical and biological properties of a cyano-based probe based on pyridazine. The ex vivo staining of Aβ plaques in APP/PS1 mice brain sections by this fluorescent probe is also presented.

2. Materials and Methods

2.1. General Experimental Methods. ^{1}H NMR spectra were recorded in $CDCl_3$ unless otherwise noted (values in ppm) using TMS as the standard with a JNM-ECA 500 spectrometer. Low resolution mass spectra were recorded using a Varian MAT 212 mass spectrometer. IR spectra (KBr) were measured with a Bruker-Vector 22 instrument (Bruker, Bremen). Flash column chromatography was performed using silica gel (70–230 mesh). All reagent-grade chemicals were purchased from Sigma-Aldrich (St. Louis, MO, USA), and synthetic Aβ_{42} peptide was purchased from rPeptide (Bogart, GA, USA).

*2.2. Synthesis and Characterization of Catechol Aldehyde (**2**).* A mixture of **1** (300 mg, 0.97 mmol), 3,4-dihydroxybenzaldehyde (147 mg, 1.06 mmol), and K_2CO_3 (293 mg, 2.12 mmol) was dissolved in DMF (20 ml) and refluxed for 24 h. After evaporating the solvent under reduced pressure, H_2O (100 ml) and methylene chloride (50 ml) were added. The organic layer was separated and dried over $MgSO_4$. The pure product (**2**) was obtained by column chromatography on silica gel using CH_2Cl_2 as the eluent. Yield: 89%. IR (KBr) = 3091, 2920, 2852, 1691, 1671, 1647, 1605, 1590, 1526, 1499, 1364, 1280, 1188. ^{1}H NMR ($CDCl_3$) = 9.83 (s, 1H), 8.01 (d, 1H, J = 13.75 Hz), 7.67 (s, 1H), 7.54–7.38 (m, 4H), 7.18–6.99 (m, 2H), 6.69 (d, 2H, J = 8.70 Hz), 2.98 (S, 6H). MS (EI) m/z 375 $[M]^+$, 188, 159, 145, 117.

2.3. Synthesis and Characterization of Probe **3**. A mixture of **2** (100 mg, 0.27 mmol) and cyanoacetic acid (30 mg, 0.36 mmol) was vacuum dried, and $CHCl_3$ (50 ml) and piperidine were added. The solution was refluxed for 15 h. Then, H_2O (50 ml) was added. The organic layer was separated and dried over $MgSO_4$. The pure product (**3**) was obtained by column chromatography on silica gel (CH_2Cl_2: MeOH = 6 : 1). Yield: 58%. IR (KBr) = 3398, 3091, 2922, 2853, 2211, 1651, 1632, 1603, 1524, 1503, 1363, 1335, 1277, 1187, 1163, 1125. ^{1}H-NMR ($CDCl_3$) = 8.04 (d, 1H, J = 6.86 Hz), 7.81 (d, 1H, J = 14.25 Hz), 7.80 (s, 1H), 7.55–7.51 (m, 2H), 7.37–7.33 (dd, 2H, J = 8.56, 8.52 Hz), 7.18–7.09 (m, 1H), 6.99 (d, 1H, J = 14.29 Hz), 6.66 (d, 2H, J = 7.42 Hz), 2.89 (S, 6H). MS (EI) m/z 398 $[M\text{-}CO_2]^+$, 382, 256, 145, 129, 111, 97, 83, 78, 63.

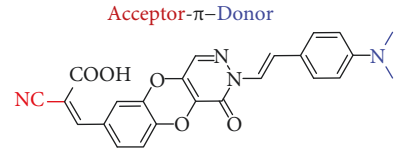

Figure 1: Chemical structure of fluorescent probe **3**.

2.4. UV/VIS and Fluorescence Analysis. UV/VIS and fluorescence spectra were recorded and analyzed. For the UV/VIS spectra, an Infinite M200 Pro Microplate reader (Tecan, Switzerland) equipped with cells with a 1.0 cm path length was used. The scan rate was 120 nm/min. The excitation and emission λ_{max} values of probe **3** (10 μM) were recorded with a detector (slit of 1 mm) and a data interval of 5 nm in DMF.

2.5. Preparation of Aβ42 *Aggregates and Fluorescence Spectrum Measurement.* Aggregated Aβ peptide was prepared by diluting Aβ42 to a final concentration of 100 μM in PBS (pH 7.4). This solution was incubated at 200 rpm and 37°C for 3 days. The formation of Aβ fibrils was confirmed by ThT assay. The excitation and emission λ_{max} values of probe **3** were measured using an Infinite M200 Pro Microplate reader (Tecan, Switzerland) equipped with a detector (slit 1 mm) with a data interval of 5 nm. The scan rate was 120 nm/min. Probe **3** (10 μM) was reacted with and without 20 μM Aβ aggregates for 20 min in PBS at 37°C. The emission spectra and fluorescence intensity of the samples were measured. The fold increase was calculated by comparing the fluorescence intensity with and without 20 μM Aβ aggregates.

2.6. Binding Constant (K_D) Measurement. A 10 μM solution of aggregated Aβ42 was combined with probe **3** (0.1, 0.5, 1, 2, 5, and 10 μM) in PBS (pH 7.4). The solutions were incubated for 10 min at 37°C, and then their fluorescence intensity was determined at 408 nm (excitation wavelength). K_D was determined as described previously [25].

*2.7. Lipophilicity (*log *P).* Probe **3** was added to a premixed suspension containing 500 μL of octanol and 500 μL of PBS solution, and the resulting suspension was vortexed vigorously for 10 min and centrifuged at 3000 rpm for 5 min. Two layers separated out, and 100 μL aliquots from octanol and the PBS solution layers were removed and analyzed for their fluorescence intensity. The log *P* value was calculated as the logarithm of the ratio of the fluorescence intensity in octanol versus that in PBS solution.

2.8. Maestro Images Analysis. An optical data study was performed using a Maestro 2.0 in vivo imaging system. The images were acquired as described previously [25]. Solutions of probe **3** (1 μM) were prepared with and without 20 μM Aβ aggregates in PBS. Fluorescence emission was obtained by analyzing the resulting images with commercial software (Maestro™ 2.4).

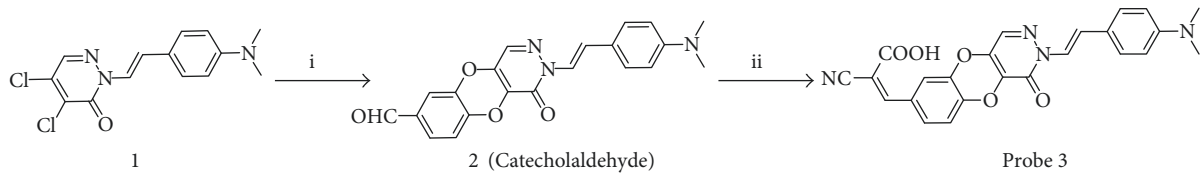

Scheme 1: Reaction scheme for the synthesis of the pyridazine-based probe (**3**). (i) DMF, 3,4-dihydroxybenzaldehyde, K_2CO_3, refluxed for 24 h; (ii) $CHCl_3$, cyanoacetic acid, piperidine, refluxed for 15 h.

2.9. Histological Costaining with Aβ Antibody and Probe **3**. The brain from 12-month-old transgenic APP/PS1 mice was removed and cut into 5 μm sections. The mouse brain sections were stained with probe **3** and anti-Aβ using the following method: first, the brain sections were equilibrated in PBS solution for 10 min, washed with PBS containing 0.1% Tween 20 (PBS-T) and 5% BSA for 30 min, and washed again with PBS-T supplemented with 1% BSA for 5 min 3 times. Second, the washed sections were incubated with primary antibody (rabbit anti-Aβ, 1 : 100 dilution in PBS-T supplemented with 1% BSA) overnight at 4°C, washed with PBS-T supplemented with 1% BSA 3 times, and stained with secondary antibody (Alexa 555 goat antirabbit IgG, 1 : 100 dilution in PBS-T supplemented with 1% BSA). After washing with PBS, the prestained sections were stained with 10 μM probe **3** for 30 min. The stained section was washed with PBS and analyzed under an FV1000D (Olympus, Tokyo, Japan) confocal laser scanning microscope.

3. Results and Discussion

The synthesis of probe **3** is outlined in Scheme 1. First, commercially available 3,4-dihydroxybenzaldehyde was converted to the corresponding catechol aldehyde (**2**) by reacting it with compound **1**. The Knövenagel condensation of compound **2** with cyanoacetic acid afforded the final fluorescent probe (**3**).

The optical properties of the synthesized fluorescent probe (**3**) with aggregated Aβ42 peptides in PBS (pH 7.4) were analyzed, and the results are shown at Table 1. Probe **3** exhibited an excitation maximum at 408 nm and an emission maximum at 670 nm (Table 1 and Figure 2).

To operate as a fluorescent probe targeting Aβ plaques, a compound must show a significant rise in fluorescence intensity upon binding with Aβ aggregates compared to the fluorescence intensity of free Aβ aggregates in solution [15]. Therefore, we compared the fluorescence intensity of probe **3** to the fluorescence intensity of the probe in the presence of Aβ aggregates (Figure 3(a)). As shown in Table 1, we observed a remarkable increase (35-fold) in the fluorescence intensity of probe **3** in the presence of Aβ aggregates. Additionally, the gain in fluorescence intensity was visually confirmed using a Maestro fluorescence imaging system (Figure 3(c)). This effect is due to conformational changes: When the probe in solution with Aβ aggregates is in the unbound state, free rotation through a single bond is permitted, whereas upon binding to Aβ aggregates, the probe exhibits a significant increase in fluorescence intensity due to restricted movement [26]. The binding of probe **3** to Aβ aggregates was also accompanied by a blueshift in the emission spectrum [15]. The emission wavelength of probe **3** exhibited significant blueshifts (66 nm, Table 1), indicating that probe **3** likely intercalated into the hydrophobic pocket of the Aβ aggregates. This result suggested that probe **3** could be "turned on" via an increase in fluorescence intensity and a blueshift in its emission wavelength upon interacting with Aβ aggregates.

Next, we measured the apparent binding constant (K_D) of fluorescent probe **3** to Aβ aggregates. The fluorescence intensity of solutions of probe **3** at various concentrations in the presence of Aβ aggregates was measured, revealing that the K_D value of probe **3** was 0.35 ± 0.03 μM (Table 1 and Figure 3(b)). This binding constant was significantly higher than that of our previously reported fluorescence probe, probe **1** (1.83 ± 0.31 μM) [24]. The lipophilicity (log *P*) of probe **3** was also evaluated to determine whether it could permeate through the blood brain barrier (BBB). The log *P* value of probe **3** was found to be 2.94 (Table 1), suggesting that probe **3** has desirable properties regarding BBB permeability [21].

Table 1: Fluorescence profile and K_D and log *P* values of probe **3** with Aβ aggregates.

Optical properties	Probe **3**
λ_{ex} (nm)	408
λ_{em} (nm)	670
$\lambda_{ex}/\lambda_{em}$ with Aβ (nm)	408/604
Fold increase with Aβ	34.92
K_D (mean ± SD) (μM)	0.35 ± 0.03
log *P* (lipophilicity)	2.94

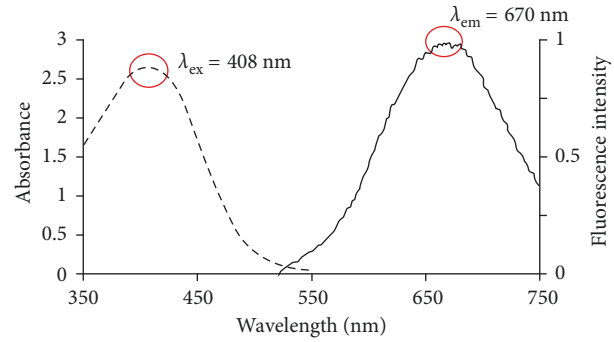

Figure 2: Absorbance and emission spectra of probe **3** in DMF. The maximum wavelengths in the absorbance and emission spectra are 408 nm and 670 nm, respectively.

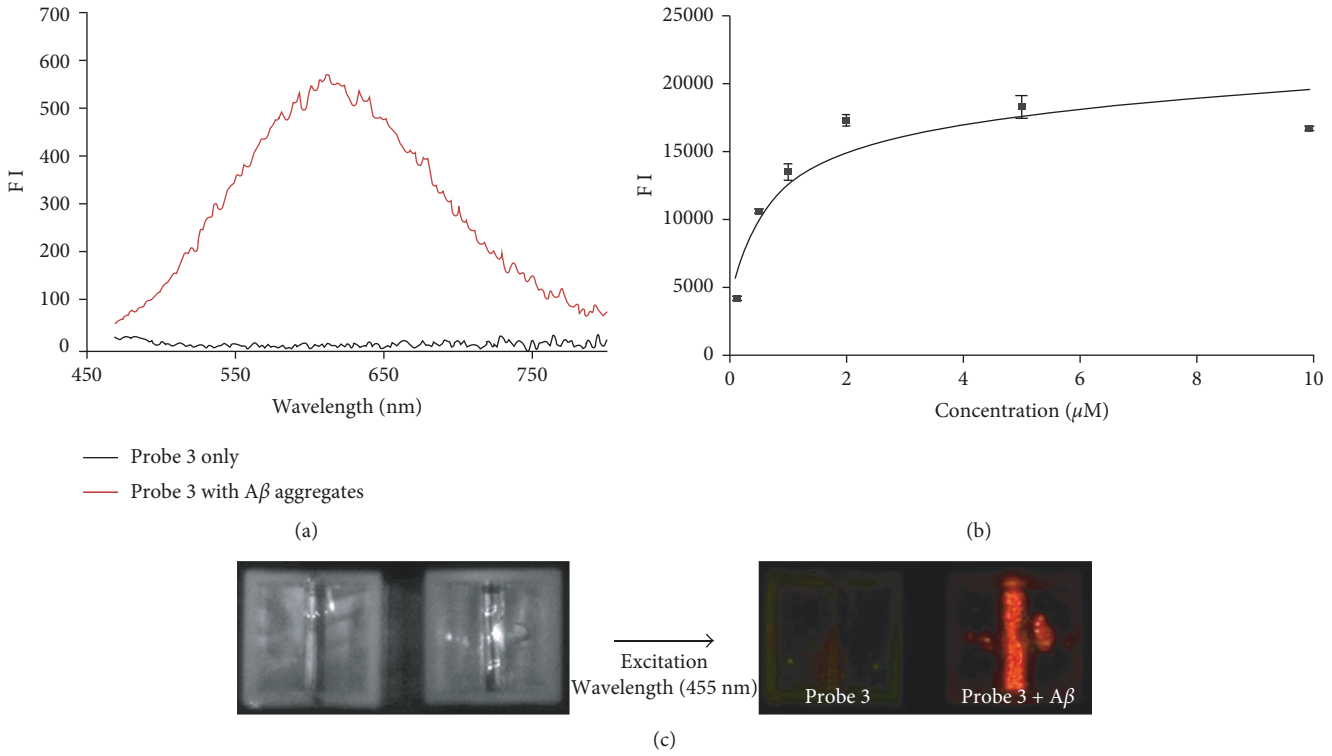

FIGURE 3: Emission spectra of probe **3** in the presence and absence of Aβ aggregates (a) and a plot of the fluorescence intensity (at $\lambda_{em} = 604$) as a function of the concentration of probe **3** in the presence of Aβ aggregates (10 μM) in PBS (b). The apparent dissociation constant (K_D) was 0.35 ± 0.03 μM. (c) Imaging of the fluorescence intensity of probe **3** and Aβ42 aggregates using a Maestro imaging system.

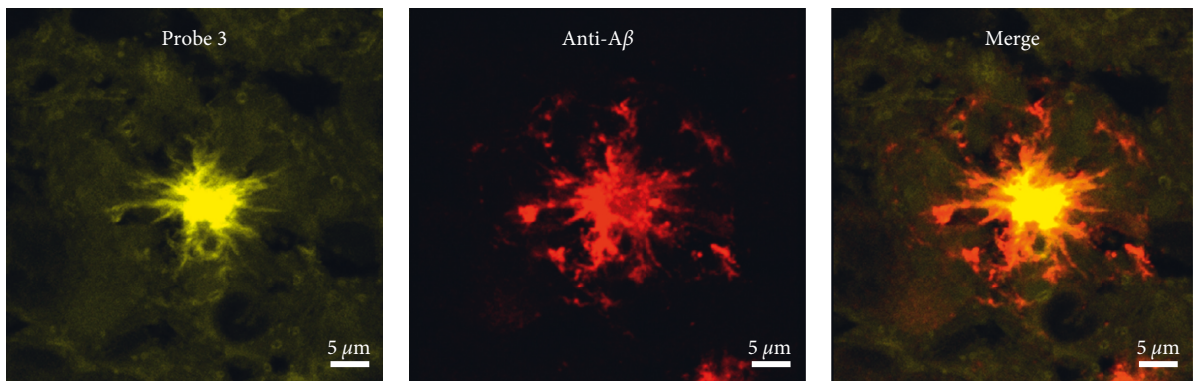

FIGURE 4: Histological double staining of 5 μm double sections from the cortex of APP/PS1 mouse brains with probe **3** and anti-Aβ. All of the images were acquired at a certain excitation wavelength (anti-Aβ: 555 nm and probe **3**: 408 nm) by a confocal laser scanning microscope.

The probe developed in this paper, probe **3**, meets the requirements for a fluorescence imaging probe for AD: high fluorescence receptivity, strong binding affinity, and hydrophobicity. To assess whether fluorescent probe **3** could stain Aβ plaques in mouse brain tissue, we further evaluated the histological costaining of Aβ plaques in APP/PS1 mouse brain sections with probe **3** and anti-Aβ. Aβ plaques in the mouse brain section were identified by staining with anti-Aβ as a control. As shown in Figure 4, the brain section exposed to probe **3** exhibited significant fluorescence. Notably, the merged images showed colocalization of the areas stained with probe **3** and anti-Aβ, which demonstrates the selective targeting of Aβ plaques by probe **3**.

4. Conclusions

In summary, we successfully synthesized probe **3** as a novel Aβ plaque-targeting fluorescent probe by applying the concept of a donor-π-acceptor structure to the scaffold of a previously reported pyridazine dye, probe **1**. Probe **3** exhibited a strong fluorescence response ($F_{A\beta}/F_0 > 34$-fold), high affinity for Aβ42 aggregates ($K_D = 0.35 \pm 0.03$ μM), and

sufficient hydrophobicity to penetrate the BBB (log $P = 2.94$). Furthermore, probe **3** specifically stained the Aβ plaques in APP/PS1 mouse brain sections. These results indicate probe **3** as a novel fluorescence imaging agent for the study of AD.

Conflicts of Interest

The authors declare that they have no conflicts of interest.

Acknowledgments

This project was supported by the Ministry of Science and ICT (MIST), Republic of Korea.

References

[1] G. Edwards III, I. Moreno-Gonzalez, and C. Soto, "Amyloid-beta and tau pathology following repetitive mild traumatic brain injury," *Biochemical and Biophysical Research Communications*, vol. 483, no. 4, pp. 1137–1142, 2017.

[2] E. D. Roberson and L. Mucke, "100 years and counting: prospects for defeating Alzheimer's disease," *Science*, vol. 314, no. 5800, pp. 781–784, 2006.

[3] J. H. Kim, J. Lee, S. Lee, and E. J. Cho, "Quercetin and quercetin-3-**β**-d-glucoside improve cognitive and memory function in Alzheimer's disease mouse," *Applied Biological Chemistry*, vol. 59, no. 5, pp. 721–728, 2016.

[4] C. A. Mathis, Y. Wang, and W. E. Klunk, "Imaging beta-amyloid plaques and neurofibrillary tangles in the aging human brain," *Current Pharmaceutical Design*, vol. 10, no. 13, pp. 1469–1492, 2004.

[5] A. Nordberg, "PET imaging of amyloid in Alzheimer's disease," *The Lancet Neurology*, vol. 3, no. 9, pp. 519–527, 2004.

[6] D. J. Selkoe, "Imaging Alzheimer's amyloid," *Nature Biotechnology*, vol. 18, no. 8, pp. 823-824, 2000.

[7] E. D. Agdeppa, V. Kepe, J. Liu et al., "Binding characteristics of radiofluorinated 6-dialkylamino-2-naphthylethylidene derivatives as positron emission tomography imaging probes for beta-amyloid plaques in Alzheimer's disease," *Journal of Neuroscience*, vol. 21, no. 24, p. RC189, 2001.

[8] H. F. Kung, S. R. Choi, W. Qu, W. Zhang, and D. Skovronsky, "18F stilbenes and styrylpyridines for PET imaging of A**β** plaques in Alzheimer's disease: a miniperspective," *Journal of Medicinal Chemistry*, vol. 53, no. 3, pp. 933–941, 2010.

[9] C. A. Mathis, Y. Wang, D. P. Holt, G. F. Huang, M. L. Debnath, and W. E. Klunk, "Synthesis and evaluation of 11C-labeled 6-substituted 2-arylbenzothiazoles as amyloid imaging agents," *Journal of Medicinal Chemistry*, vol. 46, no. 13, pp. 2740–2754, 2003.

[10] N. Okamura, Y. Shiga, S. Furumoto et al., "In vivo detection of prion amyloid plaques using [(11)C]BF-227 PET," *European Journal of Nuclear Medicine and Molecular Imaging*, vol. 37, no. 5, pp. 934–941, 2010.

[11] M. Ono, A. Wilson, J. Nobrega et al., "11C-labeled stilbene derivatives as A**β**-aggregate-specific PET imaging agents for Alzheimer's disease," *Nuclear Medicine and Biology*, vol. 30, no. 6, pp. 565–571, 2003.

[12] C. C. Rowe, U. Ackerman, W. Browne et al., "Imaging of amyloid beta in Alzheimer's disease with 18F-BAY94-9172, a novel PET tracer: proof of mechanism," *The Lancet Neurology*, vol. 7, no. 2, pp. 129–135, 2008.

[13] Z. P. Zhuang, M. P. Kung, A. Wilson et al., "Structure-activity relationship of imidazo[1,2-a]pyridines as ligands for detecting beta-amyloid plaques in the brain," *Journal of Medicinal Chemistry*, vol. 46, no. 2, pp. 237–243, 2003.

[14] R. Weissleder and U. Mahmood, "Molecular imaging," *Radiology*, vol. 219, no. 2, pp. 316–333, 2001.

[15] W. M. Chang, M. Dakanali, C. C. Capule, C. J. Sigurdson, J. Yang, and E. A. Theodorakis, "ANCA: a family of fluorescent probes that bind and stain amyloid plaques in human tissue," *ACS Chemical Neuroscience*, vol. 2, no. 5, pp. 249–255, 2011.

[16] G. Yu, H. Jung, and H. Mok, "Indocyanine green-incorporated exosomes for improved in vivo imaging of sentinel lymph node," *Applied Biological Chemistry*, vol. 59, no. 1, pp. 71–76, 2016.

[17] M. Hintersteiner, A. Enz, P. Frey et al., "In vivo detection of amyloid-beta deposits by near-infrared imaging using an oxazine-derivative probe," *Nature Biotechnology*, vol. 23, no. 5, pp. 577–583, 2005.

[18] E. E. Nesterov, J. Skoch, B. T. Hyman, W. E. Klunk, B. J. Bacskai, and T. M. Swager, "In vivo optical imaging of amyloid aggregates in brain: design of fluorescent markers," *Angewandte Chemie International Edition*, vol. 44, no. 34, pp. 5452–5456, 2005.

[19] S. B. Raymond, J. Skoch, I. D. Hills, E. E. Nesterov, T. M. Swager, and B. J. Bacskai, "Smart optical probes for near-infrared fluorescence imaging of Alzheimer's disease pathology," *European Journal of Nuclear Medicine and Molecular Imaging*, vol. 35, no. S1, pp. S93–S98, 2008.

[20] Q. Li, J. S. Lee, C. Ha et al., "Solid-phase synthesis of styryl dyes and their application as amyloid sensors," *Angewandte Chemie International Edition*, vol. 43, no. 46, pp. 6331–6335, 2004.

[21] C. Ran, X. Xu, S. B. Raymond et al., "Design, synthesis, and testing of difluoroboron-derivatized curcumins as near-infrared probes for in vivo detection of amyloid-beta deposits," *Journal of the American Chemical Society*, vol. 131, no. 42, pp. 15257–15261, 2009.

[22] M. Ono, M. Ishikawa, H. Kimura et al., "Development of dual functional SPECT/fluorescent probes for imaging cerebral beta-amyloid plaques," *Bioorganic and Medicinal Chemistry Letters*, vol. 20, no. 13, pp. 3885–3888, 2010.

[23] W. E. Klunk, H. Engler, A. Nordberg et al., "Imaging brain amyloid in Alzheimer's disease with Pittsburgh Compound-B," *Annals of Neurology*, vol. 55, no. 3, pp. 306–319, 2004.

[24] Y. D. Park, J. H. Park, M. G. Hur et al., "Fluorescent 2-styrylpyridazin-3(2H)-one derivatives as probes targeting amyloid-beta plaques in Alzheimer's disease," *Bioorganic and Medicinal Chemistry Letters*, vol. 22, no. 12, pp. 4106–4110, 2012.

[25] S. J. Jung, S. H. Park, E. J. Lee et al., "Development of fluorescent probes that bind and stain amyloid plaques in Alzheimer's disease," *Archives of Pharmacal Research*, vol. 38, no. 11, pp. 1992–1998, 2015.

[26] M. Staderini, M. A. Martin, M. L. Bolognesi, and J. C. Menendez, "Imaging of beta-amyloid plaques by near infrared fluorescent tracers: a new frontier for chemical neuroscience," *Chemical Society Reviews*, vol. 44, no. 7, pp. 1807–1819, 2015.